

ROBUST ASYMMETRIC LEARNING IN POMDPs

A PREPRINT

Andrew Warrington^{*1}, J. Wilder Lavington^{*2}, Adam Ścibior², Mark Schmidt^{2,3}, and Frank Wood^{2,4}

¹Department of Engineering Science, University of Oxford

²Department of Computer Science, University of British Columbia

³Alberta Machine Learning Intelligence Institute (AMII)

⁴Montréal Institute for Learning Algorithms (MILA)

ABSTRACT

Policies for partially observed Markov decision processes can be efficiently learned by imitating policies for the corresponding fully observed Markov decision processes. Unfortunately, existing approaches for this kind of imitation learning have a serious flaw: the expert does not know what the trainee cannot see, and so may encourage actions that are sub-optimal, even unsafe, under partial information. We derive an objective to instead train the *expert* to maximize the expected reward of the imitating *agent* policy, and use it to construct an efficient algorithm, adaptive asymmetric DAgger (A2D), that jointly trains the expert and the agent. We show that A2D produces an expert policy that the agent can safely imitate, in turn outperforming policies learned by imitating a fixed expert.

1 Introduction

Consider a version of the stochastic shortest path problem (Bertsekas & Tsitsiklis, 1991) where an *agent* learns to cross a frozen lake and avoid patches of weak ice. The agent can either cross the ice directly, or take a longer, safer route circumnavigating the lake. In this environment, the agent is provided aerial images of the lake, which include color variations at patches of weak ice. To successfully cross the lake, the agent must learn to identify its own position, goal position, and the weak ice from the images. Even for this simple environment, high-dimensional inputs and sparse rewards can make learning a suitable policy computationally expensive and sample inefficient. Therefore one might instead efficiently learn, in simulation, an omniscient *expert* policy, conditioned on a low-dimensional vector which fully describes the state of the simulator, to complete the task. The agent (conditioned on images) then learns to mimic expert actions using sample-efficient imitation learning (Ross et al., 2011). This yields a high-performing agent conditioned on images at test time acquired with fewer environment interactions overall compared to direct reinforcement learning.

In this paper, we address the task of learning a policy to maximize expected reward of a partially observed Markov decision processes (POMDPs) (Åström, 1965; Lovejoy, 1991; Littman, 2009) in the presence of additional information from the simulator as in the example above. We first considering solving for the optimal policy under full information, referred to as the *expert*, by operating directly on a Markov decision process (MDP) (Sutton, 1992). We then replicate this policy with a second policy, referred to as the *agent*, which is only conditioned on partial information. This approach takes advantage of efficient methods for solving MDPs to learn the expert, and efficient imitation learning algorithms (Ross et al., 2011) to learn the agent. By exploiting this asymmetry we can learn expert *and* agent with lower overall cost, compared to learning the agent directly through reinforcement.

While intuitively appealing, imitation learning can fail in asymmetric environments. Consider now that the image of the lake does not indicate the location of the weak ice. The agent is now operating under uncertainty, resulting in a different optimal policy. Imitating the expert forces the agent to always cross the lake, even though the agent cannot locate the weak ice, and hence cannot avoid it like the expert would. Even though the expert is optimal under the MDP, it provides poor supervision to the agent, in that imitation learning does not yield a policy that is optimal under partial information.

The key insight from this simple example is that *the expert has no knowledge of what the agent does not know*. As such, the expert cannot provide suitable supervision, and proposes actions that are not robust to the increased uncertainty of partial information. The main algorithmic contribution we present follows directly from this insight: **one must refine the expert based on the observed performance of the agent imitating it.**

* Indicates equal contribution. Correspondence to andreww@robots.ox.ac.uk.

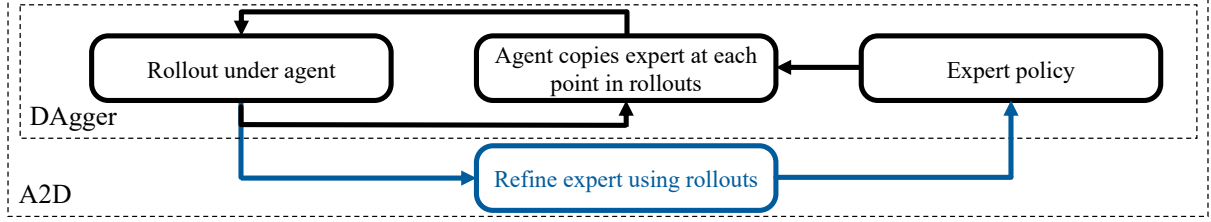


Figure 1: Flow chart describing adaptive asymmetric DAgger (A2D) introduced in this work, which builds on DAgger (Ross et al., 2011) by further refining the expert conditioned on the agent policy.

In this work we consider the use of asymmetric information in imitation and reinforcement learning. Here asymmetric information is defined as additional information available during training that will not be available at test time. We first frame the use of asymmetric information in imitation learning as an amortized posterior inference task. We then demonstrate how naive imitation approaches can fail. To address this failure we present a new algorithm: adaptive asymmetric DAgger (A2D), building on our key insight that the expert should be trained to maximize the expected reward of the agent that imitates it, as illustrated in Figure 1. We begin by showing that the agent solves a posterior inference task, targeting the action of the expert while marginalizing the over the true state conditioned on the current observed state. We then show we are able to pass a policy gradient, with respect to the reward of the agent, through this inference task to the parameters of the expert policy, and that we can construct a tractable estimator of this policy gradient. Our A2D algorithm then interleaves RL updates to the expert using this policy gradient, with standard imitation learning to update the agent. Under mild assumptions, we show theoretically, and then verify empirically, that A2D modifies the expert policy such that the optimal agent policy can be recovered through imitation. Crucially, A2D can be integrated with a variety of different RL algorithms, avoids taking expensive and high-variance RL steps in the agent policy, and does not require any pretrained artifacts or example trajectories.

2 Background

2.1 Optimality and Markov Decision Processes

We define a Markov decision process (MDP), $\mathcal{M}_\Theta(\mathcal{S}, \mathcal{A}, \mathcal{R}, \mathcal{T}_0, \mathcal{T}, \Pi_\Theta)$, as a random process which produces a sequence of tuples $\tau_t := \{a_t, s_t, s_{t+1}, r_t\}$, for a particular set of states $s_t \in \mathcal{S}$, actions $a_t \in \mathcal{A}$, initial state distribution $p(s_0) \in \mathcal{T}_0$, transition distribution $p(s_{t+1}|s_t, a_t) \in \mathcal{T}$, reward function $r_t : \mathcal{S} \times \mathcal{A} \times \mathcal{S} \rightarrow \mathbb{R}$, and policy $\pi_\theta \in \Pi_\Theta : \mathcal{S} \rightarrow \mathcal{A}$ parameterized by θ . The generative model, shown in Figure 2, for this finite horizon process is defined as:

$$q_{\pi_\theta}(\tau) = p(s_{0:T+1}, a_{0:T}) = p(s_0) \prod_{t=0}^T p(s_{t+1}|s_t, a_t) \pi_\theta(a_t|s_t). \quad (1)$$

where we also denote the marginal distribution with respect to a state s , under trajectory distribution given in (1), as $q_{\pi_\theta}(s)$. Reinforcement learning then seeks to recover the policy which maximizes the expected reward over a trajectory, $\theta^* = \arg \max_{\theta \in \Theta} \mathbb{E}_{q_{\pi_\theta}} [\sum_{t=0}^T r_t(s_t, a_t, s_{t+1})]$. We also consider an extension of this framework to infinite time horizons, where we instead maximize the non-stationary, infinite horizon discounted return. This optimization problem can be described more succinctly as:

$$\theta^* = \min_{\theta \in \Theta} \mathbb{E}_{s \sim d^{\pi_\theta}, a \sim \pi_\theta} [Q^{\pi_\theta}(a, s)] \quad \text{where} \quad d^{\pi_\theta}(s) = (1 - \gamma) \sum_{t=0}^{\infty} \gamma^t q_{\pi_\theta}(s_t = s), \quad (2)$$

$$\text{and} \quad Q^{\pi_\theta}(a, s) = \mathbb{E}_{s' \sim p(s'|s, a)} [r(s, a, s') + \gamma \mathbb{E}_{a' \sim \pi_\theta} [Q^{\pi_\theta}(a', s')]], \quad (3)$$

where the distribution over states, $d^{\pi_\theta}(s)$, will be referred to as the *state occupancy*.

2.2 State Estimation and Partially Observed Markov Decision Processes

Partially observed Markov decision processes (POMDPs) extend MDPs by instead observing a random variable conditioned on the state, $o_t \in \mathcal{O}$, $o_t \sim p(\cdot|s_t)$. The agent samples actions conditioned on all previous observations and actions: $\pi_\phi(a_t|a_{0:t-1}, o_{0:t})$. In practice however one can introduce an intermediate belief state $b_t \in \mathcal{B}$ generated from estimating the sufficient statistics of the true state distribution then sampling from this estimate. This separates the task of state-estimation and policy learning into two distinct problems, that are individually more manageable. This means that we can first learn an estimate of the state, which the policy is then conditioned on: $\pi_\phi \in \Pi_\Phi : \mathcal{B} \rightarrow \mathcal{A}$ (Kaelbling

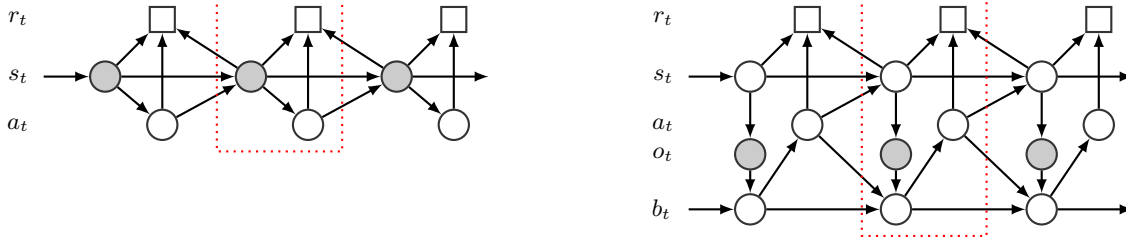


Figure 2: Graphical models of an MDP (left) and a POMDP (right). State transition dynamics, $p(s_t|s_{t-1}, a_t)$, reward function, $R(s_t, a_t, s_{t+1})$, and initial state distribution, $p(s_0)$, are identical for both.

et al., 1998). The resulting stochastic process, denoted $\mathcal{M}_\Phi(\mathcal{S}, \mathcal{O}, \mathcal{B}, \mathcal{A}, \mathcal{R}, \mathcal{T}_0, \mathcal{T}, \Pi_\Phi)$, generates a sequence of tuples $\tau_t = \{a_t, b_t, o_t, s_t, s_{t+1}, r_t\}$. We wish to find a policy, $\pi_{\phi^*} \in \Pi_\Phi$, which maximizes the expected reward under this new generative model (shown graphically in Figure 2):

$$q_{\pi_\phi}(\tau) = p(s_0) \prod_{t=0}^T p(s_{t+1}|s_t, a_t) p(b_t|b_{t-1}, o_t, a_{t-1}) p(o_t|s_t) \pi_\phi(a_t|b_t). \quad (4)$$

Throughout this paper we use q_π as general notation for the trajectory generation process, indicating which policy is used to generate the rollout as a subscript. We indicate whether the trajectory includes the belief state by subscripting with a policy that is conditioned on belief state ($\pi_\phi, \hat{\pi}_\theta, \pi_\psi, \pi_\eta$ and π_β in this paper). Policies conditioned on state (π_θ in this paper) also follow this convention. In this setting the belief state can be interpreted as the distribution over states, given the observations received and actions taken up to time t , and is updated recursively using new observations and actions (Igl et al., 2018; Rodriguez et al., 2000; Littman & Sutton, 2002; Doshi-Velez et al., 2013). In practice an explicit belief state is often replaced with a fixed-length window of observations and actions $b_t := (o_{t-w:t}, a_{t-w:t-1})$, where the window length is $w \in \mathbb{Z}_{>0}$ (Murphy, 2000; Laskin et al., 2020), such that the policy is conditioned on a fixed-dimensional variable: $a_t \sim \pi_\phi(a_t|o_{t-w:t}, a_{t-w:t-1})$. We define the occupancy measure, $d^{\pi_\phi}(s, b)$, as the marginal distribution of $q_{\pi_\phi}(\tau)$ with respect to s and b . The occupancies $d^{\pi_\phi}(s)$ and $d^{\pi_\phi}(b)$ are then themselves marginals of $d^{\pi_\phi}(s, b)$. Finally, throughout this work we discuss *MDP-POMDP pairs*. These “paired processes” are defined by an MDP tuple and POMDP tuple that have identical state transition dynamics, reward generating functions and initial state distributions. While taking advantage of this relationship is desirable, these process pairs can and often do have different optimal policies. We will comment more on this in the following section.

2.3 Imitation Learning

While RL presents one avenue to arrive at an optimal policy (which maximizes reward), another option is also sometimes available. Imitation learning (IL) assumes access to either an expert policy capable of solving a task or a set of example trajectories generated by such an expert. When provided with example trajectories, the agent is learned through regressing onto the example actions of the expert. However, the learned agent policy can perform arbitrarily poorly in states not in the training set (Laskey et al., 2017). Instead, online IL algorithms, such as DAgger (Ross et al., 2011), assume access to a performant expert that can be queried across the entire state-space. DAgger interacts with the environment under a mixture policy π_β between the expert policy π_θ and the current agent policy π_ϕ . Here the mixture coefficient β is annealed to zero during training, so that examples from the environment are eventually drawn from the distribution over states induced by the agent policy. This allows supervision to be given for states actually visited by the agent policy, and avoids a compounding model error that grows with the time-horizon. The DAgger solution can be written as:

$$\phi^* = \arg \min_{\phi} \mathbb{E}_{s_t \sim d^{\pi_\beta}} [\mathbb{KL}[\pi_\theta(a_t|s_t) || \pi_\phi(a_t|s_t)]], \quad \text{where } \pi_\beta = \beta \pi_\theta + (1 - \beta) \pi_\phi, \quad (5)$$

While IL approaches can provide higher sample-efficiency than RL approaches, they require access to either an expert or expert trajectories and thus are not always applicable.

2.4 Asymmetric Information

However, in many environments additional information is available during training that can be exploited to accelerate learning (Vapnik & Vashist, 2009; Pinto et al., 2017). This additional information is often referred to as *asymmetric information*. A common example of this is the availability of a compact and complete state representation at training time (such as a RAM state), but only noisy or incomplete observation at test time (such as an image). Pinto et al. (2017) exploit this asymmetry by learning a value function conditioned on a compact state, but a policy conditioned on the

Algorithm 1 Asym DAGger (AD)

```

1: Input: POMDP  $\mathcal{M}_\Phi$ , expert  $\pi_\theta(a_t|s_t)$ , Annealing
   schedule  $\text{AnnealBeta}(n, \beta)$ .
2: Return: Agent policy parameters  $\psi$ .
3:  $\psi \leftarrow \text{InitNet}(\mathcal{M}_\Phi)$ 
4:  $\beta \leftarrow 1$ ,  $D \leftarrow \emptyset$ 
5: for  $n = 0, \dots, N$  do
6:    $\beta \leftarrow \text{AnnealBeta}(n, \beta)$ 
7:    $\pi_\beta \leftarrow \beta\pi_\theta + (1 - \beta)\hat{\pi}_\psi$ 
8:    $\mathcal{T} = \{\tau_i\}_{i=1}^T \sim q_{\pi_\beta}(\tau)$ 
9:    $D \leftarrow \text{UpdateBuffer}(D, \mathcal{T})$ 
10:
11:
12:    $\psi \leftarrow \text{ProjectStep}(D, \pi_\theta, \hat{\pi}_\psi)$ 
13: end for
14: return  $\psi$ 

```

Algorithm 2 Adaptive Asym DAGger (A2D)

```

1: Input: MDP  $\mathcal{M}_\Theta$ , POMDP  $\mathcal{M}_\Phi$ , Annealing schedule
    $\text{AnnealBeta}(n, \beta)$ .
2: Return: Agent policy parameters  $\psi$ .
3:  $\theta, \psi, \nu_m, \nu_p \leftarrow \text{InitNets}(\mathcal{M}_\Theta, \mathcal{M}_\Phi)$ 
4:  $\beta \leftarrow 1$ ,  $D \leftarrow \emptyset$ 
5: for  $n = 0, \dots, N$  do
6:    $\beta \leftarrow \text{AnnealBeta}(n, \beta)$ 
7:    $\pi_\beta \leftarrow \beta\pi_\theta + (1 - \beta)\hat{\pi}_\psi$ 
8:    $\mathcal{T} = \{\tau_i\}_{i=1}^T \sim q_{\pi_\beta}(\tau)$ 
9:    $D \leftarrow \text{UpdateBuffer}(D, \mathcal{T})$ 
10:    $V^{\pi_\beta} \leftarrow \beta V_{\nu_m}^{\pi_\theta} + (1 - \beta)V_{\nu_p}^{\hat{\pi}_\psi}$ 
11:    $\theta, \nu_m, \nu_p \leftarrow \text{RLStep}(\mathcal{T}, V^{\pi_\beta}, \pi_\beta)$ 
12:    $\psi \leftarrow \text{ProjectStep}(D, \pi_\theta, \hat{\pi}_\psi)$ 
13: end for
14: return  $\psi$ 

```

Figure 3: Algorithms for asymmetric DAGger (left) and our algorithm adaptive asymmetric DAGger (right). The additional steps we introduce are highlighted in blue, and implement the additional feedback loop in Figure 1.

noisy observations actually available at test time. In this setting, the value function is not required at test-time and can thus be discarded after training. Gradients for this asymmetric actor critic algorithm can then be computed as:

$$U(\phi) = \mathbb{E}_{a \sim \pi_\phi, b \sim d^{\pi_\phi}} \left[\sum_{t=0}^{\infty} \gamma^t r_t \right], \quad \nabla_\phi U(\phi) \approx \mathbb{E}_{s_t, b_t \sim d^{\pi_\phi}} \left[\mathbb{E}_{a_t \sim \pi_\phi(\cdot|b_t)} [A^{\pi_\phi}(s_t, a_t) \nabla_\phi \log \pi_\phi(a_t|b_t)] \right], \quad (6)$$

$$\text{where } Q^{\pi_\phi}(a, s) = \mathbb{E}_{s' \sim p(s'|s, a)} [r(s, a, s') + \gamma V^{\pi_\phi}(s')], \quad V^{\pi_\phi}(s) = \mathbb{E}_{a \sim \pi_\phi} [Q^{\pi_\phi}(a, s)] \quad (7)$$

and the *advantage* is defined as $A^{\pi_\phi}(s_t, a_t) = Q^{\pi_\phi}(a_t, s_t) - V^{\pi_\phi}(s_t)$. These methods often outperform “symmetric” RL as the function approximators are simpler to tune, provide better gradient signal to the policy, and are computationally cheaper. Other approaches have been used in pretraining an encoder transforming high-dimensional observations targeting the low-dimensional state representation (Levine et al., 2016; Finn et al., 2016; Andrychowicz et al., 2020). Beyond this, asymmetric and imitation learning themes have been used in variety scenarios, such as using ensembles of policies (Song et al., 2019), imitating a low-dimensional attention-based representation (Salter et al., 2019), multi-objective reinforcement learning (Schwab et al., 2019), or through the use of privileged information dropout (Kamienny et al., 2020; Lambert et al., 2018), while Arora et al. (2018) identify a scenario where a using privileged information is ineffective. Notably, online imitation learning is also naturally suited to asymmetric environments (Chen et al., 2020; Pinto et al., 2017), where the expert acts on true state information:

$$\phi^* \in \arg \min_\phi \mathbb{E}_{s_t, b_t \sim d^{\pi_\beta}} [\mathbb{KL}[\pi_\theta(a_t|s_t) || \pi_\phi(a_t|b_t)]], \quad \text{where } \pi_\beta = \beta\pi_\theta + (1 - \beta)\pi_\phi. \quad (8)$$

As the expert is not used at test time, the expert can use asymmetric information to simplify learning (Pinto et al., 2017), or, enable more effective data augmentation (Chen et al., 2020).

3 Asymmetric Imitation Learning as Posterior Inference

Our ultimate objective is to derive an update that can be applied to the expert, such that application of an imitation learning recovers the optimal agent policy. This avoids taking high variance RL steps in the agent directly, and instead leverages the sample efficiency of IL. We begin by studying the asymmetric IL (AIL) objective in (8). We show that the minimizer of this objective is equal to the solution of a posterior inference problem. We refer to this solution as the *implicit agent policy*:

Definition 1 (Implicit Agent Policy). *For any fully observable policy π_θ and any policy π_η we define*

$$\hat{\pi}_\theta^\eta(a_t|b_t) := \mathbb{E}_{s_t \sim d^{\pi_\eta}(s_t|b_t)} [\pi_\theta(a_t|s_t)], \quad (9)$$

and say that $\hat{\pi}_\theta^\eta$ is the implicit agent policy of π_θ under π_η . When $\pi_\eta = \hat{\pi}_\theta^\eta$, we write the latter as $\hat{\pi}_\theta$ and refer to it as the implicit agent policy of π_θ .

This defines a posterior predictive density, which integrates out all knowledge of the underlying true state distribution using the true marginal distribution over states given belief states. This distribution represents the agent policy that minimizes the divergence between actions taken by the agent and the expert for a given state and belief state pair. To prove this we substitute this definition into the objective defined in (8), defined in the following theorem.

Theorem 2 (Asymmetric IL Target). *For any fully observable policy π_θ and any fixed policy π_η , the implicit agent policy $\hat{\pi}_\theta^\eta$ minimizes the following asymmetric imitation learning objective:*

$$\hat{\pi}_\theta^\eta(a_t|b_t) = \arg \min_{\pi \in \Pi_\Phi} \mathbb{E}_{s_t, b_t \sim d^{\pi_\eta}} [\mathbb{KL} [\pi_\theta(a_t|s_t) || \pi(a_t|b_t)]] . \quad (10)$$

Proof. An extended version of this proof is included in Appendix C.2.

$$\begin{aligned} \mathbb{E}_{s_t, b_t \sim d^{\pi_\eta}} [\mathbb{KL} [\pi_\theta(a_t|s_t) || \pi(a_t|b_t)]] &= \mathbb{E}_{b_t \sim d^{\pi_\eta}} [\mathbb{E}_{s_t \sim d^{\pi_\eta}(a_t|b_t)} [\mathbb{E}_{a_t \sim \pi_\theta} [\log \pi(a_t|b_t)]]] + K \\ &= \mathbb{E}_{b_t \sim d^{\pi_\eta}} [\mathbb{E}_{a_t \sim \hat{\pi}_\theta^\eta} [\log \pi(a_t|b_t)]] + K = \mathbb{E}_{b_t \sim d^{\pi_\eta}} [\mathbb{KL} [\hat{\pi}_\theta^\eta(a_t|b_t) || \pi(a_t|b_t)]] + K' \end{aligned}$$

Since $\hat{\pi}_\theta^\eta \in \Pi_\Phi$, it follows that

$$\hat{\pi}_\theta^\eta = \arg \min_{\pi \in \Pi_\Phi} \mathbb{E}_{b_t \sim d^{\pi_\eta}} [\mathbb{KL} [\hat{\pi}_\theta^\eta(a_t|b_t) || \pi(a_t|b_t)]] = \arg \min_{\pi \in \Pi_\Phi} \mathbb{E}_{s_t, b_t \sim d^{\pi_\eta}} [\mathbb{KL} [\pi_\theta(a_t|s_t) || \pi(a_t|b_t)]] . \quad \square \quad (11)$$

However, using the implicit agent policy directly, as defined in (9), is intractable, as we are unable to sample from $d^{\pi_\eta}(s_t|b_t)$. Therefore, asymmetric imitation learning fits a variational approximation to the implicit agent policy, denoted $\pi_\psi(a_t|b_t)$, in the objective in (11):

$$\psi^* = \arg \min_{\psi \in \Psi} F(\psi) = \arg \min_{\psi \in \Psi} \mathbb{E}_{s_t, b_t \sim d^{\pi_\eta}} [\mathbb{KL} [\pi_\theta(a_t|s_t) || \pi_\psi(a_t|b_t)]] , \quad (12)$$

$$\Rightarrow \nabla_\psi F(\psi) = -\mathbb{E}_{s_t, b_t \sim d^{\pi_\eta}} [\mathbb{E}_{a_t \sim \pi_\theta(a_t|s_t)} [\nabla_\psi \log \pi_\psi(a_t|b_t)]] , \quad (13)$$

where we include the derivation in full in the appendix. As with many variational objectives, this conveniently side-steps needing to sample from the conditional distribution. Then if the variational family, Π_ψ , is sufficiently expressive, the divergence between the implicit agent policy and the variational approximation goes to zero. In online imitation learning it is common to roll out under the agent policy, which is equivalent to setting $\pi_\eta = \pi_{\psi^*}$. In this case finding a variational policy is equivalent to solving a simple fixed point equation. Under standard assumptions we show in Appendix 5 that such a fixed point equation converges to the correct target distribution. In practice, we also find that this iterative scheme tends to converge, even in the presence of inexact intermediate updates.

4 Failure of Imitation Learning

However, there is a critical flaw with the methodology described above. While the divergence between the implicit agent policy and the variational approximation may go to zero as the agent policy is trained, there is no guarantee that the minimum divergence between the implicit agent policy and the expert policy in (10) is zero. This means that even a perfect variational agent might be not able to faithfully reproduce the expert actions in the asymmetric setting. As a result, policies with a non-zero divergence between the optimal fully observed policy and its implicit agent policy may incur arbitrarily low reward.

To demonstrate this failure, we introduce two gridworld environments, shown in Figure 4. Both require the agent (red) to navigate to a goal (green) while avoiding a hazard (blue). The agent is conditioned on an image of the environment where the hazard is not visible, while the expert is conditioned on a compact omniscient state vector. Every movement made incurs a base reward of -2 . The first environment, referred to as “frozen lake” (as described in the introduction, shown in Figure 4a) places the hazard (weak ice) in a random location in the interior nine squares. The expert crosses the ice directly, avoiding the weak patch, earning an average reward of 10.66. The agent should go around the environment, guaranteeing avoidance of the patch, and earning a reward of 4. The implicit agent policy averages the expert actions over the location of the weak patch, resulting in a policy that always goes straight across the ice. This policy hits the patch in one third of trials, earning an average reward of -26.6 , representing a catastrophic failure. The second example is a gridworld embedding of the classic Tiger Door problem (Littman et al., 1995), where the positions of the hazard and goal are unknown, but become visible if the agent pushes a button (pink). Pushing the button does not directly incur a negative reward directly, but, does require the agent to make more moves, and hence indirectly incurs a reward of -4 . The expert goes straight to the goal, earning a reward of 6, whereas the agent should always press the button, and then proceed to the now-visible goal, earning a reward of 2. The implicit agent policy averages over the location of the goal, and *never* presses the button, incurring a reward of -54 , again, representing a catastrophic failure.

Results are shown in Figure 4, and confirm our intuitions: RL in the MDP (RL (MDP)) is stable and efficient, whereas RL directly in the image-based POMDP (RL and RL (Asym)) is slow and sample inefficient. Asymmetric IL (AD) converges almost immediately, but converges to a sub-optimal solution as expected.

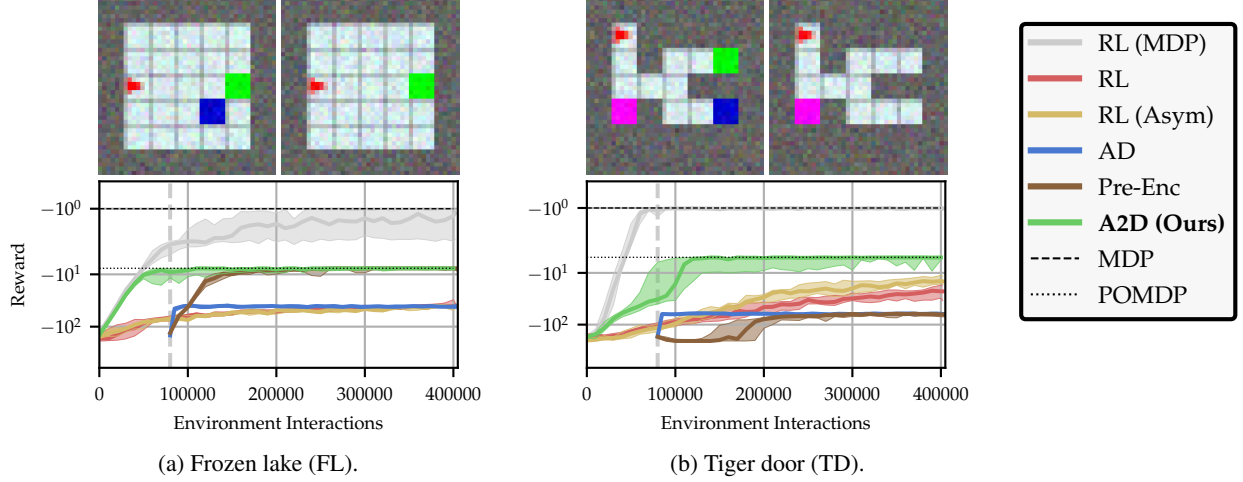


Figure 4: Results for application of the methods discussed to two gridworld environments. TRPO (Schulman et al., 2015a) is used for RL methods. Marked in broken lines are the optimal reward for the MDP and POMDP, normalized so the optimal MDP reward is -1 . All policies (except RL (MDP)) are conditioned on image-based input. A2D reliably finds the optimal POMDP policy, in a sample budget commensurate with the MDP, whereas other methods yield unreliable results. AD and Pre-Enc begin when the MDP has converged, as this is the required expenditure for these methods. Pre-Enc represents using a pretrained encoder converting the partial observation into a low-dimensional estimate of the state, trained on rollouts obtained from the MDP. The encoder is then frozen and RL steps are taken in the low-dimensional encoded representation. Experimental configurations, additional results and discussions are included in the appendix.

Using our intuition from these experiments and insight from Theorem 2 we are able to define a property of an MDP-POMDP pair that guarantees imitation learning to succeed. We refer to this property as *identifiability*.

Definition 3 (Identifiable Processes). *Given an MDP \mathcal{M}_Θ , and POMDP \mathcal{M}_Φ pair, with optimal MDP policy $\pi_{\theta^*} \in \Pi_{\Theta^*} \subseteq \Pi_\Theta$, and implicit agent policy $\hat{\pi}_{\theta^*}$, we call the pair $\{\mathcal{M}_\Theta, \mathcal{M}_\Phi\}$ as **identifiable** if and only if $\mathbb{E}_{s_t, b_t \sim d^{\hat{\pi}_{\theta^*}}} [\mathbb{KL} [\pi_{\theta^*}(a_t|s_t) || \hat{\pi}_{\theta^*}(a_t|b_t)]] = 0, \forall \theta^* \in \Theta^*, t \in \{0, \dots, \infty\}$.*

When this condition is satisfied, under standard assumptions, 8 is guaranteed to yield the optimal partially observed policy (as shown in Appendix 5). When this condition is not satisfied, as in the case in the two gridworlds introduced above, the reward earned by the agent may be arbitrarily sub-optimal. Unfortunately, this definition represents a fixed property of two stochastic processes (e.g. the MDP-POMDP pair). We therefore target a relaxation of this property through manipulation of the experts Q-function, to ensure that the agent can perfectly imitate the expert and recover the optimal partially observed agent policy.

5 Correcting Asymmetric IL: Adaptive Asymmetric DAGger

We use the theoretical insight from Section 3 and practical insight from Section 4 to construct an on-policy reinforcement learning update applied to the expert policy, instead maximizing the reward under the implicit agent policy, such that subsequent application of imitation learning will recover the desired agent. This update is the core contribution of the method we present, adaptive asymmetric DAGger (A2D). A2D extends DAGger by interleaving such a policy update to the expert with imitation updates to the agent.

5.1 Updating The Expert

To derive the update applied to the expert, π_θ , we first define the expected reward under the corresponding implicit agent policy, $\hat{\pi}_\theta$:

$$J(\theta) = \mathbb{E}_{a, b \sim \hat{\pi}_\theta, d^{\hat{\pi}_\theta}} [Q^{\hat{\pi}_\theta}(a, b)], \quad \text{where} \quad Q^{\hat{\pi}_\theta}(a, b) = \mathbb{E}_{b', s' \sim p(\cdot|a, b)} [r(s, a, s') + \gamma \mathbb{E}_{a' \sim \hat{\pi}_\theta} [Q^{\hat{\pi}_\theta}(a', b')]]. \quad (14)$$

This objective defines the reward of the agent in terms of the parameters of the expert policy, such that maximizing $J(\theta)$ maximizes the reward obtained by the implicit agent policy. We consider optimization of a lower bound of the true policy gradient, where by at each stage we seek to obtain improvement under a behavioral policy as in Williams (1992); Schulman et al. (2015a, 2017). Under exact updates, the sequence of policies would represent taking the softmax

optimal policy (Levine, 2018; Haarnoja et al., 2018) of the objective for a single step, and then reverting back to the previous policy for the remaining steps. In this case, the behavioral policy is defined as our variational agent policy, π_ψ , which is then trained using the imitation learning objective from (10). We are now able pass the gradient operator through the expectation and rearrange:

$$\nabla_\theta J_\psi(\theta) = \nabla_\theta \mathbb{E}_{a_t, b_t \sim \pi_\theta, d^{\pi_\psi}} [Q^{\pi_\psi}(a_t, b_t)] = \mathbb{E}_{b_t \sim d^{\pi_\psi}} [\nabla_\theta \mathbb{E}_{s_t \sim d^{\pi_\psi}(s_t|b_t)} [\mathbb{E}_{a_t \sim \pi_\theta} [Q^{\pi_\psi}(a_t, b_t)]]], \quad (15)$$

$$= \mathbb{E}_{s_t, b_t \sim d^{\pi_\psi}} [\mathbb{E}_{a_t \sim \pi_\theta} [Q^{\pi_\psi}(a_t, b_t) \nabla_\theta \log \pi_\theta(a_t|s_t)]] , \quad (16)$$

$$= \mathbb{E}_{s_t, b_t, a_t \sim d^{\pi_\psi}(s_t, b_t) \pi_\psi(a_t|b_t)} \left[\frac{\pi_\theta(a_t|s_t)}{\pi_\psi(a_t|b_t)} Q^{\pi_\psi}(a_t, b_t) \nabla_\theta \log \pi_\theta(a_t|s_t) \right] , \quad (17)$$

where a complete derivation is included in the appendix. This estimator allows us to **apply updates to the expert, that maximize the agent reward**, by alternating between applying updates to improve the expert under the agents reward, and then bringing the agent back towards the expert using supervised learning. Since the form of the expert update is similar to a standard RL update, A2D is compatible with most RL algorithms. The performance of such REINFORCE based estimators can be improved by using a learned baseline to reduce variance (Williams, 1992). When the value function is used as the baseline, the resulting value is referred to as the *advantage*, $A^\pi(a_t, b_t) = Q^\pi(a_t, b_t) - V^\pi(b_t)$, with corresponding gradient update:

$$\nabla_\theta J_\psi(\theta) = \mathbb{E}_{s_t, b_t, a_t \sim d^{\pi_\psi}(s_t, b_t) \pi_\psi(a_t|b_t)} \left[\frac{\pi_\theta(a_t|s_t)}{\pi_\psi(a_t|b_t)} A^{\pi_\psi}(a_t, b_t) \nabla_\theta \log \pi_\theta(a_t|s_t) \right] . \quad (18)$$

This update is the core of the A2D algorithm. There are, however, important considerations about how the Q-function can be estimated, and, when explicitly approximating the Q-function can be avoided entirely.

5.2 Estimating the Q-Function

All the terms in (17) and (18) can be computed directly with the exception of the Q-function, and the thus advantage. One approach is to train an additional function approximator targeting the Q values directly, and a second estimator targeting the value function, such that these can be used together to estimate the advantage without directly using the Monte Carlo rollouts. While from the theoretical perspective this is preferable for A2D, this approach can lead to unstable and biased training by overly relying on imperfect function approximators, and, increases the computational cost. Therefore, instead, Monte Carlo estimations of the Q-value can be calculated directly from the rollouts, increasing variance but reducing bias. However, and somewhat unexpectedly, this approach can fail in A2D. This can be shown by expanding the definition of Q in terms of state:

$$Q^{\pi_\psi}(a, b) = \mathbb{E}_{s' \sim p(\cdot|a, b)} [\mathbb{E}_{b' \sim d^{\pi_\psi}(b'|s')} [r(s, a, s') + \gamma \mathbb{E}_{a' \sim \pi_\psi} [Q^{\pi_\psi}(a', b')]]] . \quad (19)$$

Since sampling from $d^{\pi_\psi}(b'|s')$ is intractable, our only option is to use the same sample throughout, $b' = b$. Using single-sample estimates of the outer expectation, where the belief state used is the same as in the gradient evaluation in (18), biases the gradient estimator by re-using random variables. This corresponds to the gradient estimator *not* being conditionally independent of the current (unobserved) state given the belief state. This introduces a correlation that essentially allows the expert to cheat by exclusively using the true state for a single time step of a rollout. This is illustrated in Figure 5a, which shows a tiger door environment that can be completed in one step with omniscient information. Using a single trajectory per state doesn't necessary allow the marginalization over possible states given the belief state. This effect is observed when we don't approximate Q directly, as the expert learns a poor solution, effectively optimizing the reward of the MDP. However, when a Q-function is learned, this marginalization is performed by the Q-function and the correct solution is recovered.

Practically, we note that when the Q-function is not required, faster and more reliable convergence is achieved by not estimating the Q-function. Therefore, our "default" A2D algorithm does not use the Q-function, citing faster convergence, lower computational cost, fewer hyperparameters, and more stable learning. Additionally, a performance gap and non-zero KL divergence between the expert and the agent policies can be used as an instrument for indicating when the Q-function should be learned. Lastly, similar to DAgger, we gather environment examples under a mixture policy $\pi_\beta(a_t|s_t, b_t) = \beta \pi_\theta(a_t|s_t) + (1 - \beta) \pi_\psi(a_t|b_t)$. In this case, the Q-function and value functions are defined as $Q^{\pi_\beta}(a_t, s_t, b_t)$ and $V^{\pi_\beta}(a_t, s_t, b_t)$ respectively. Like DAgger, the mixture coefficient β is annealed from one to zero during training. The final gradient estimator we use in all experiments where the Q-function is not explicitly learned uses generalized advantage estimation (Schulman et al., 2015b), and is given as:

$$\nabla_\theta J_\psi(\theta) = \mathbb{E}_{s_t, b_t, a_t \sim d^{\pi_\beta}(s_t, b_t) \pi_\beta(a_t|s_t, b_t)} \left[\frac{\pi_\theta(a_t|s_t)}{\pi_\beta(a_t|s_t, b_t)} \hat{A}^{\pi_\beta}(a_t, s_t, b_t) \nabla_\theta \log \pi_\theta(a_t|s_t) \right] , \quad (20)$$

$$\text{where } \hat{A}^{\pi_\beta}(a_t, s_t, b_t) = \sum_{t=0}^{\infty} (\gamma \lambda)^t \delta_t, \text{ and } \delta_t = r_t + \gamma V^{\pi_\beta}(s_{t+1}, b_{t+1}) - V^{\pi_\beta}(s_t, b_t), \quad (21)$$

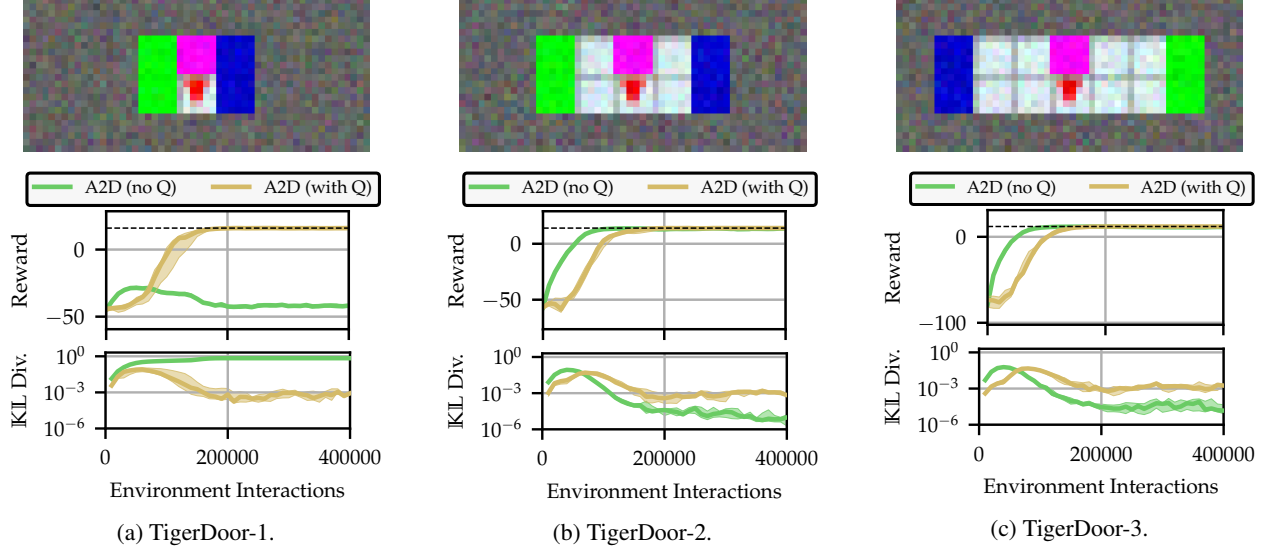


Figure 5: Results for investigating the use of a Q-function, as introduced in Section 5. In both cases a value function is used as a baseline (c.f. (18)). The Q-function is learned using (19), targeting the expected discounted sum of rewards ahead conditioned on a particular action, and is then used to estimate the gradient without direct use of Monte Carlo rollouts. When no Q-function is being used, the advantage is computed using GAE (c.f. (20) and (21)). Mean and quartiles across 10 random seeds are shown. *Left*: Training curves for the original Tiger Door problem. A2D does not converge to the correct policy as predicted if a Q-function is not simultaneously learned. This poor performance is clarified by the high KL-divergence during training. If a Q-function is learned, the desired behavior is recovered. *Middle and Right*: Separating the goal by at least one square means desired behavior is recovered regardless of whether a Q-function is used. However, convergence is slower when using a Q-function.

5.3 A2D: Adaptive Asymmetric Dagger

We now have all the required steps to build the full A2D algorithm, as shown in Algorithm 2:

1. **Gather data** (Alg. 2, Ln 8): Collect samples by rolling out under the variational agent policy (or mixture policy) by sampling trajectories from $q_{\pi_\beta}(\tau)$ as defined in (4).
2. **Refine Expert** (Alg. 2, Ln 10, 11): Apply a policy gradient update step to the expert using an importance weighted advantage as per (20). Any policy gradient update (such as TRPO or PPO) can be used in this step. This step updates the expert policy parameters (θ), the agent value function parameters (ν_p), and the expert value function parameters (ν_m). The agent is not updated, which can be easily implemented by freezing the value of ψ (a standard autodiff operation).
3. **Update Agent** (Alg. 2, Ln 12): Perform an imitation step to fit the variational agent policy to the expert, using (13), identical to the supervised learning step used by DAgger. This step uses the divergence between the policies, can be performed until convergence using cross-validation to avoid over-fitting and can safely use a replay buffer to improve data efficiency, all reducing the amount of hyperparameter tuning required.

6 Revisiting Frozen Lake & Tiger Door

We now revisit the more complex gridworld examples introduced in Section 3 to fully evaluate A2D, the results of which are included in Figure 4. A2D converges to the optimal POMDP reward, whereas the other methods fail for one, or both, gridworlds. Further, the optimal POMDP solution is obtained in a similar number of environment interactions as the MDP. This means the agent, observing high-dimensional, partial aerial renderings, is being learned in a sample budget commensurate with the omniscient, compact-state MDP.

In Figure 6 we present several additional results derived from the two gridworld environments. In the top row, we show the evolution of the reward garnered by the expert and agent during A2D training, in parallel with the projection loss. We see that, as predicted, the projection loss grows as the expert optimizes the policy to maximize reward under the MDP, with efficiency that the agent cannot replicate. As β is annealed the expert and agent policies coalesce, as

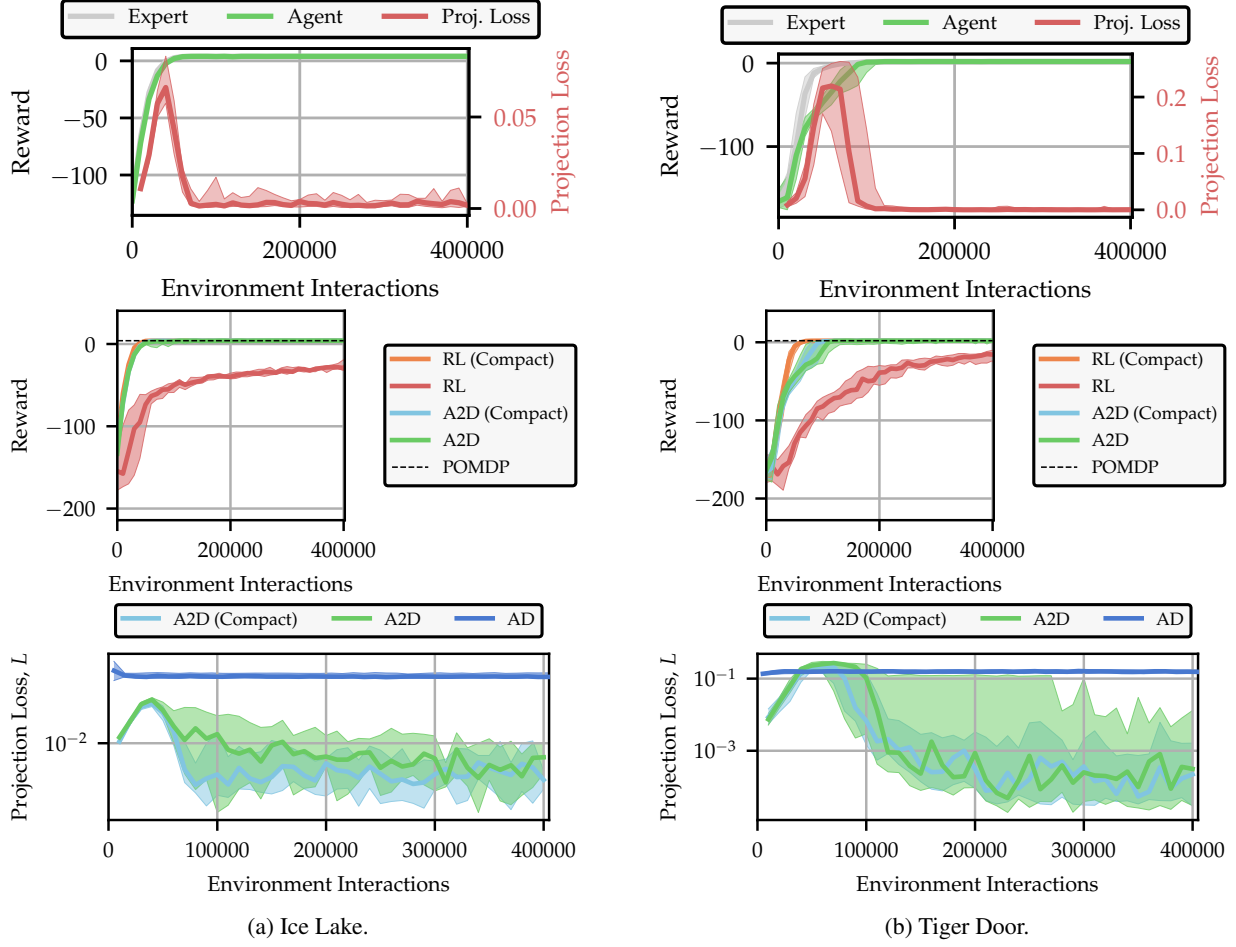


Figure 6: Additional results for the gridworld experiments presented in Figure 4. All policy gradient steps are taken using TRPO. *Top row*: Training curves for the expert and agent during A2D training, and the projection loss between the expert and agent. Due to the annealing effect of β we can see that the KL-divergence between expert and agent (projection loss) rises as the expert learns to solve the MDP, but then reduces to zero as β approaches zero and the POMDP is solved instead. Both MDP and POMDP converge to the same reward. *Middle row*: Training curves comparing convergence of A2D and vanilla RL on the POMDP for compact (one-hot vector) representations and image-based representations. We see that the RL converges quickly on the compact representation (orange) and slowly for images (red). A2D on the other hand converges in a sample complexity commensurate with operating directly on the compact MDP for both image-based and compact representations. This confirms our hypothesis that A2D can reduce the complexity of operating in high-dimensional, partially observed environments into a complexity commensurate with the best-possible convergence rate obtained by performing RL directly on the most efficient encoding. *Bottom row*: Plots showing the evolution of the projection loss for A2D using both compact and image-based representations, and AD. We see that AD saturates to a high projection loss, whereas A2D reduces to a low divergence, at similar rate, for both compact and image-based representations. Note the logarithmic y-scale.

indicated by the projection loss dropping to zero. In the second row we show the performance differential when using image-based and compact representations as input to the *agent* policy. Most importantly, we see that the performance of A2D is not greatly affected by using image-based or compact representations as input to the agent. This confirms our hypothesis that we can transfer the perception task to the imitation learning step, and solve the partially observed control task in the compact MDP space. Finally, we show the divergences between the expert policy (fixed in AD, and as the expert policy learns in A2D). We see again that AD has a high divergence, which is converged to almost immediately. Finally, the projection loss incurred by A2D is largely invariant to the representation used on input to the agent. In the appendix we demonstrate that A2D can use PPO as the RL algorithm and achieve comparable performance as TRPO, with minimal alterations to the algorithm and source code; simply replacing the call to a TRPO update step with a PPO update step.

7 Discussion

In this work we discuss learning policies in partially observed Markov decision processes, where partial, high dimensional observations make direct application of reinforcement learning expensive and unreliable. Imitation learning provides an efficient means of learning a partially observing policy, but requires a pre-existing performant expert, and critically, assumes that the expert can provide suitable supervision – a condition we formalize as identifiability. When this condition is not satisfied, the learned agent can perform arbitrarily poorly. We therefore develop adaptive asymmetric DAgger (A2D), as a method for learning in POMDPs which retains the favorable properties of imitation learning while ensuring the optimal agent policy is learned. A2D also allows the expert to be learned online with the agent and does not require any pretrained artifacts. We also discuss when it is possible to avoid directly learning the Q-function. We show experimentally that this behavior is a property of the environment, and that for some environments Monte Carlo estimation is sufficient. While this short experiment provides some intuition for when avoiding a learned a Q-function is safe, we have thus far been unable to formalize this into a precise condition, and defer such investigation to future work.

We consider A2D as a complementary method to direct RL, AD and pretrained encoders. If the observed dimension is small, direct application of RL is likely to perform well. If the observed dimension is large and a pretrained expert is available, AD may provide a highly efficient approach. If examples are available that sufficiently cover the state-space which will be visited by the optimal policy, using a pretrained encoder or behavioral cloning are both useful options. In contrast, A2D makes none of these assumptions and expedites training in environments where asymmetric information is available. We therefore argue that A2D represents a robust and efficient method for learning partially observed policies end-to-end.

8 Acknowledgements

We thank Frederik Kunstner for his invaluable discussions, and for reviewing preliminary drafts of this work. Andrew Warrington is supported by the Shilston Scholarship, Keble College, University of Oxford. J. Wilder Lavington is supported by Inverted AI. We acknowledge the support of the Natural Sciences and Engineering Research Council of Canada (NSERC), the Canada CIFAR AI Chairs Program, and the Intel Parallel Computing Centers program. This material is based upon work supported by the United States Air Force Research Laboratory (AFRL) under the Defense Advanced Research Projects Agency (DARPA) Data Driven Discovery Models (D3M) program (Contract No. FA8750-19-2-0222) and Learning with Less Labels (LwLL) program (Contract No. FA8750-19-C-0515). Additional support was provided by UBC’s Composites Research Network (CRN), Data Science Institute (DSI) and Support for Teams to Advance Interdisciplinary Research (STAIR) Grants. This research was enabled in part by technical support and computational resources provided by WestGrid (<https://www.westgrid.ca/>) and Compute Canada (www.computecanada.ca).

References

- A. Achille and S. Soatto. Information dropout: Learning optimal representations through noisy computation. *IEEE Transactions on Pattern Analysis and Machine Intelligence*, 40(12):2897–2905, Dec 2018. ISSN 1939-3539. doi: 10.1109/tpami.2017.2784440.
- O. A. M. Andrychowicz, B. Baker, M. Chociej, R. Józefowicz, B. McGrew, J. Pachocki, A. Petron, M. Plappert, G. Powell, A. Ray, J. Schneider, S. Sidor, J. Tobin, P. Welinder, L. Weng, and W. Zaremba. Learning dexterous in-hand manipulation. *International Journal of Robotics Research*, 39(1):3–20, 2020. ISSN 17413176. doi: 10.1177/0278364919887447.
- S. Arora, S. Choudhury, and S. Scherer. Hindsight is only 50/50: Unsuitability of MDP based approximate POMDP solvers for multi-resolution information gathering, 2018.
- K. J. Åström. Optimal control of markov processes with incomplete state information. *Journal of Mathematical Analysis and Applications*, 10(1):174–205, 1965.
- D. P. Bertsekas and J. N. Tsitsiklis. An analysis of stochastic shortest path problems. *Mathematics of Operations Research*, 16(3):580–595, 1991.
- D. Chen, B. Zhou, V. Koltun, and P. Krähenbühl. Learning by cheating. In *Conference on Robot Learning*, pp. 66–75. PMLR, 2020.
- F. Doshi-Velez, D. Pfau, F. Wood, and N. Roy. Bayesian nonparametric methods for partially-observable reinforcement learning. *IEEE transactions on pattern analysis and machine intelligence*, 37(2):394–407, 2013.
- A. Dosovitskiy, G. Ros, F. Codevilla, A. Lopez, and V. Koltun. CARLA: An open urban driving simulator. In *Proceedings of the 1st Annual Conference on Robot Learning*, pp. 1–16, 2017.
- C. Finn, X. Y. Tan, Y. Duan, T. Darrell, S. Levine, and P. Abbeel. Deep spatial autoencoders for visuomotor learning. *Proceedings - IEEE International Conference on Robotics and Automation*, 2016-June:512–519, 2016. ISSN 10504729. doi: 10.1109/ICRA.2016.7487173.
- T. Haarnoja, A. Zhou, K. Hartikainen, G. Tucker, S. Ha, J. Tan, V. Kumar, H. Zhu, A. Gupta, P. Abbeel, et al. Soft actor-critic algorithms and applications. *arXiv preprint arXiv:1812.05905*, 2018.
- M. Igl, L. Zintgraf, T. A. Le, F. Wood, and S. Whiteson. Deep variational reinforcement learning for POMDPs. In *Proceedings of the 35th International Conference on Machine Learning*, volume 80 of *Proceedings of Machine Learning Research*, pp. 2117–2126, Stockholmsmässan, Stockholm Sweden, 10–15 Jul 2018. PMLR.
- L. P. Kaelbling, M. L. Littman, and A. R. Cassandra. Planning and acting in partially observable stochastic domains. *Artificial intelligence*, 101(1-2):99–134, 1998.
- P.-A. Kamienny, K. Arulkumaran, F. Behbahani, W. Boehmer, and S. Whiteson. Privileged information dropout in reinforcement learning, 2020.
- B. Kang, Z. Jie, and J. Feng. Policy optimization with demonstrations. In *Proceedings of the 35th International Conference on Machine Learning*, volume 80 of *Proceedings of Machine Learning Research*, pp. 2469–2478, Stockholmsmässan, Stockholm Sweden, 10–15 Jul 2018. PMLR.
- V. Könönen. Asymmetric multiagent reinforcement learning. *Web Intelligence and Agent Systems: An international journal*, 2(2):105–121, 2004.
- J. Lambert, O. Sener, and S. Savarese. Deep learning under privileged information using heteroscedastic dropout. In *Proceedings of the IEEE Conference on Computer Vision and Pattern Recognition*, pp. 8886–8895, 2018.
- M. Laskey, J. Lee, R. Fox, A. Dragan, and K. Goldberg. Dart: Noise injection for robust imitation learning. *arXiv preprint arXiv:1703.09327*, 2017.
- M. Laskin, K. Lee, A. Stooke, L. Pinto, P. Abbeel, and A. Srinivas. Reinforcement learning with augmented data. *arXiv preprint arXiv:2004.14990*, 2020.
- S. Levine. Reinforcement learning and control as probabilistic inference: Tutorial and review, 2018.
- S. Levine, C. Finn, T. Darrell, and P. Abbeel. End-to-end training of deep visuomotor policies. *Journal of Machine Learning Research*, 17:1–40, 2016. ISSN 15337928.
- M. L. Littman. A tutorial on partially observable markov decision processes. *Journal of Mathematical Psychology*, 53(3):119–125, 2009.
- M. L. Littman and R. S. Sutton. Predictive representations of state. In *Advances in neural information processing systems*, pp. 1555–1561, 2002.

- M. L. Littman, A. R. Cassandra, and L. P. Kaelbling. Learning policies for partially observable environments: Scaling up. *Seventh International Conference on Machine Learning*, pp. 362–370, 1995. doi: 10.1016/b978-1-55860-377-6.50052-9.
- W. S. Lovejoy. A survey of algorithmic methods for partially observed Markov decision processes. *Annals of Operations Research*, 28(1):47–65, 1991.
- K. P. Murphy. A survey of POMDP solution techniques. *environment*, 2:X3, 2000.
- L. Pinto, M. Andrychowicz, P. Welinder, W. Zaremba, and P. Abbeel. Asymmetric actor critic for image-based robot learning. *arXiv preprint arXiv:1710.06542*, 2017.
- A. C. Rodriguez, R. Parr, and D. Koller. Reinforcement learning using approximate belief states. In *Advances in Neural Information Processing Systems*, pp. 1036–1042, 2000.
- S. Ross, G. J. Gordon, and J. A. Bagnell. A reduction of imitation learning and structured prediction to no-regret online learning. *Journal of Machine Learning Research*, 15:627–635, 2011. ISSN 15324435.
- S. Salter, D. Rao, M. Wulfmeier, R. Hadsell, and I. Posner. Attention-privileged reinforcement learning. *arXiv preprint arXiv:1911.08363*, 2019.
- J. Schulman, S. Levine, P. Abbeel, M. Jordan, and P. Moritz. Trust region policy optimization. In *International conference on machine learning*, pp. 1889–1897, 2015a.
- J. Schulman, P. Moritz, S. Levine, M. Jordan, and P. Abbeel. High-dimensional continuous control using generalized advantage estimation. *arXiv preprint arXiv:1506.02438*, 2015b.
- J. Schulman, F. Wolski, P. Dhariwal, A. Radford, and O. Klimov. Proximal policy optimization algorithms. *arXiv preprint arXiv:1707.06347*, 2017.
- D. Schwab, J. T. Springenberg, M. F. Martins, M. Neunert, T. Lampe, A. Abdolmaleki, T. Hertweck, R. Hafner, F. Nori, and M. A. Riedmiller. Simultaneously learning vision and feature-based control policies for real-world ball-in-a-cup. In *Robotics: Science and Systems XV, University of Freiburg, Freiburg im Breisgau, Germany, June 22-26, 2019*, 2019. doi: 10.15607/RSS.2019.XV.027.
- J. Song, R. Lanka, Y. Yue, and M. Ono. Co-training for policy learning. *35th Conference on Uncertainty in Artificial Intelligence, UAI 2019*, 2019.
- W. Sun, J. A. Bagnell, and B. Boots. Truncated horizon policy search: Combining reinforcement learning & imitation learning. *6th International Conference on Learning Representations, ICLR 2018 - Conference Track Proceedings*, pp. 1–14, 2018.
- R. Sutton. *Reinforcement Learning*. The Springer International Series in Engineering and Computer Science. Springer US, 1992. ISBN 9780792392347.
- V. Vapnik and A. Vashist. A new learning paradigm: Learning using privileged information. *Neural networks*, 22(5-6): 544–557, 2009.
- R. J. Williams. Simple statistical gradient-following algorithms for connectionist reinforcement learning. *Machine learning*, 8(3-4):229–256, 1992.

A Table of Notation

Symbol	Name	Alternative Name(s)	Type	Description
t	Time	Discrete time step	\mathbb{Z}	Discrete time step used in integration. Indexes other values.
s_t	State	Full state, compact state, omniscient state	$\mathcal{S} = \mathbb{R}^D$	State space of the MDP. Sufficient to fully define state of the environment.
o_t	Observation	Partial observation	$\mathcal{O} = \mathbb{R}^{A \times B \times \dots}$	Observed value in POMDP, emitted conditional on state. State is generally not identifiable from observation. Conditionally dependent only on state.
a_t	Action		$\mathcal{A} = \mathbb{R}^K$	Interaction made with the environment at time t .
r_t	Reward		\mathcal{R}	Value received at time t indicating performance. Maximising sum of rewards is the objective.
b_t	Belief state		\mathcal{B}	
q_π	Trajectory distribution		$\mathcal{Q} : \Pi \rightarrow (\mathcal{A} \times \mathcal{B} \times \mathcal{O} \times \mathcal{S}^2 \times \mathcal{R})^{t+1}$	Process of sampling trajectories using the policy π . If the process is fully observed $\mathcal{O} = \emptyset$.
$\tau_{0:t}$	Trajectory	Rollouts	$(\mathcal{A} \times \mathcal{B} \times \mathcal{O} \times \mathcal{S}^2 \times \mathcal{R})^{t+1}$	Sequence of tuples containing state, next state, observation, action and reward.
γ	Discount factor		$\Gamma = [0, 1]$	Factor attenuating future reward in favour of near reward.
$p(s_{t+1} s_t, a_t)$	Transition distribution	Plant model, environment	$\mathcal{T} : \mathcal{S} \times \mathcal{A} \rightarrow \mathcal{S}$	Defines how state evolves, conditional on the previous state and the action taken.
$p(o_t s_t)$	Emission distribution	Observation function	$\mathcal{Y} : \mathcal{S} \rightarrow \mathcal{O}$	Distribution over observed values conditioned on state.
$p(s_0)$	Initial state distribution	State prior	$\mathcal{T}_0 : \rightarrow \mathcal{S}$	Distribution over state at $t = 0$.
$\pi_\theta(a_t s_t)$	MDP policy	Expert, omniscient policy, asymmetric expert, asymmetric policy	$\Pi_\Theta : \mathcal{S} \rightarrow \mathcal{A}$	Distribution over actions conditioned on state. Only used in MDP.
θ	MDP policy parameters		Θ	Parameters of MDP policy. Cumulative reward is maximised over these parameters.
$\pi_\phi(a_t b_t)$	POMDP policy	Agent, partially observing policy	$\Pi_\Phi : \mathcal{B} \rightarrow \mathcal{A}$	Distribution over actions conditioned on belief state. Only used in POMDP.
ϕ	POMDP policy parameters		Φ	Parameters of MDP policy. Cumulative reward is maximised over these parameters.
$\pi_\psi(a_t b_t)$	Variational agent policy	Variational approximation	$\Pi_\Psi : \mathcal{B} \rightarrow \mathcal{A}$	Variational approximation of the implicit agent policy.
ψ	Variational agent policy parameters		Ψ	Parameters of the variational approximation of the implicit agent policy.
π_β	Mixture policy		$\Pi_\beta : \mathcal{S} \times \mathcal{B} \rightarrow \mathcal{A}$	Mixture of MDP policy (π_θ) and POMDP policy (π_ϕ).
β	Mixing coefficient		$[0, 1]$	Fraction of MDP policy used in mixture policy.
\mathcal{D}	Replay buffer	Data buffer	$\mathcal{D} = \{\tau_{0:T_n}\}_{n \in 1:N}$	Store to access previous trajectories. Facilitates data re-use.
\mathbb{L}	Loss	Reconstruction error		Loss minimised in learning a function approximation. Manually specified and tuned.
\mathbb{D}	Divergence			Divergence measure between two probability distributions.
$\mathbb{KL}[p q]$	Kullback–Leibler divergence	KL divergence, forward KL, mass-covering KL		Particular divergence between two distributions. Forward KL is mass covering. Reverse KL ($\mathbb{KL}[q p]$) is mode seeking.
$Q^\pi(s_t, a_t)$	Q-function	State Q-function	$\mathcal{Q}_s : \mathcal{S} \times \mathcal{A} \rightarrow \mathbb{R}$	Expected sum of rewards ahead, garnered by taking action a_t in state s_t induced by policy π .
$Q^\pi(b_t, a_t)$	Belief state Q-function		$\mathcal{Q}_b : \mathcal{B} \times \mathcal{A} \rightarrow \mathbb{R}$	Expected sum of rewards ahead, garnered by taking action a_t in belief state b_t induced by policy π .
$\hat{\pi}_\theta(a_t b_t)$	Implicit agent policy		$\Pi_\Phi : \mathcal{B} \rightarrow \mathcal{A}$	Agent policy obtained by marginalising over state given belief state. Closest approximation of π_θ under partial observability. Approximated by π_ϕ .
$\hat{Q}^{\pi_\phi}(s_t, a_t)$	Belief-marginal function	Q-function	$\mathcal{Q}_s : \mathcal{S} \times \mathcal{A} \rightarrow \mathbb{R}$	Q-function, conditioned on state, obtained by rolling out under belief-state conditioned policy π_ϕ .
$d^\pi(s_t, b_t)$	Occupancy		$M : \mathcal{S} \times \mathcal{B} \rightarrow \mathbb{R}$	Joint density of $s_t = s$ and $b_t = b$ given policy π . Marginal of q_π over previous and future states, belief states, and all actions, observations and rewards.
π_η	Fixed reference distribution		Π	Fixed distribution that is rolled out under to generate samples that are used in gradient calculation.

Table 1: Notation and definitions used throughout this paper.

B Additional Experimental Information

We also include results in Figure 7 using PPO (Schulman et al., 2017) as the policy gradient update used in A2D, instead of TRPO. All curves use image-based inputs. We see that PPO actually diverges for image-based inputs, but that A2D converges to the desired solution, again in commensurate time with when TRPO is used in A2D. This highlights how A2D is largely agnostic to the policy gradient method used to update the expert policy. As such, we do not suggest that A2D is a “better RL algorithm,” but is instead a way of formulating a problem such that the favorable properties of imitation learning and RL (operating on MDPs) are both retained.

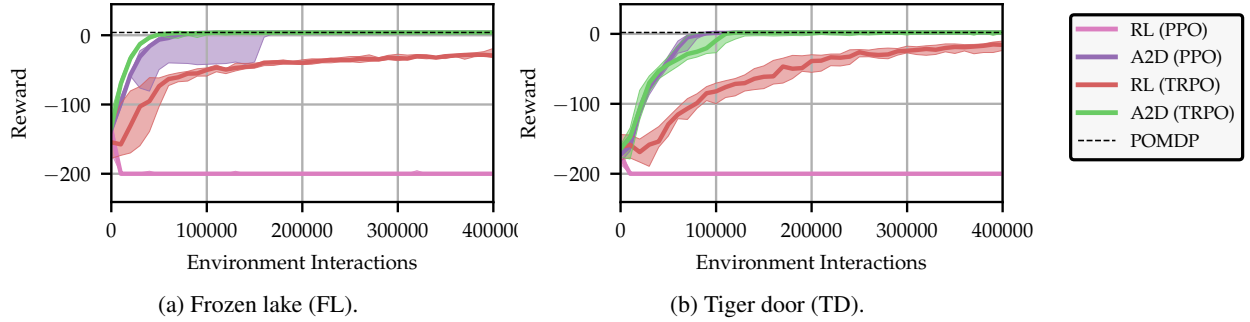


Figure 7: Results for using PPO (Schulman et al., 2017) on the two gridworld environments across ten random seeds, compared with TRPO. We see that PPO diverges for image-based representations (pink), but functions as intended when used in A2D with image-based representations (purple), only lagging slightly behind the performance of the MDP. This shows that A2D can be used, with minimal modifications, with a range of policy-gradient based RL algorithms. We use a learning rate of $7e-3$ for learning all function approximators, a batch and buffer size of 2,000 samples, an entropy regularizer of 0.001 applied to the surrogate loss, and decayed β at a rate of 0.8.

Finally we include additional results in Figure 8 showing the evolution of the expert and agent during training, across the three Tiger Door environments introduced in Figure 5. We see that learning the Q-function learns the correct behavior in all scenarios, but with slower convergence and a more variable optimization path.

C Additional Proofs

In this section we provide full proofs for the theorems and derived expressions presented in the main text.

C.1 Occupancy Measures

Throughout this paper we use $q_\pi(\tau)$ as general notation for the trajectory generation process, indicating which policy is used to generate the rollout as a subscript (c.f. (1) and (4)). We define $d^\pi(s_t, b_t)$, referred to as the occupancy measure, as the time-marginal of $q_\pi(\tau)$, marginalizing over time and all variables in the trajectory other than s_t and b_t :

$$d^\pi(s_t, b_t) = \frac{1}{T} \sum_{t=0}^T \int_{o_{0:T}, r_{0:T}, a_{0:T}} \int_{s_{0:T \setminus t}} \int_{b_{0:T \setminus t}} q_\pi(\tau) db_{0:T \setminus t} ds_{0:T \setminus t} do_{0:T} dr_{0:T} da_{0:T}, \quad (22)$$

$$d^\pi(s_t) = \int_{b \in \mathcal{B}} d^\pi(s_t, b) db, \quad d^\pi(s_t | b_t) = \int_{b \in \mathcal{B}} d^\pi(s_t, b) \delta(b_t - b) db, \quad (23)$$

$$d^\pi(b_t) = \int_{s \in \mathcal{S}} d^\pi(s, b_t) ds, \quad d^\pi(b_t | s_t) = \int_{s \in \mathcal{S}} d^\pi(s, b_t) \delta(s_t - s) ds. \quad (24)$$

Despite the complex form of this expression, we can sample from $d^\pi(s_t, b_t)$ very simply by rolling out under the policy π according to $q_\pi(\tau)$ and taking the t^{th} state-belief state pair, where t is sampled from a uniform distribution. This is a sample from the joint, $p(s_t, b_t)$, and so we can also recover a *single* sample from the conditional density $d^\pi(s_t | b_t)$ for the sampled b_t by taking the associated s_t (and vice-versa for conditioning on s_t). Sampling multiple states from this distribution conditioned on a specific b_t value is intractable. Indeed, much of the technical work presented is casting the task such that we can use samples from the joint in-place of samples from the conditional.

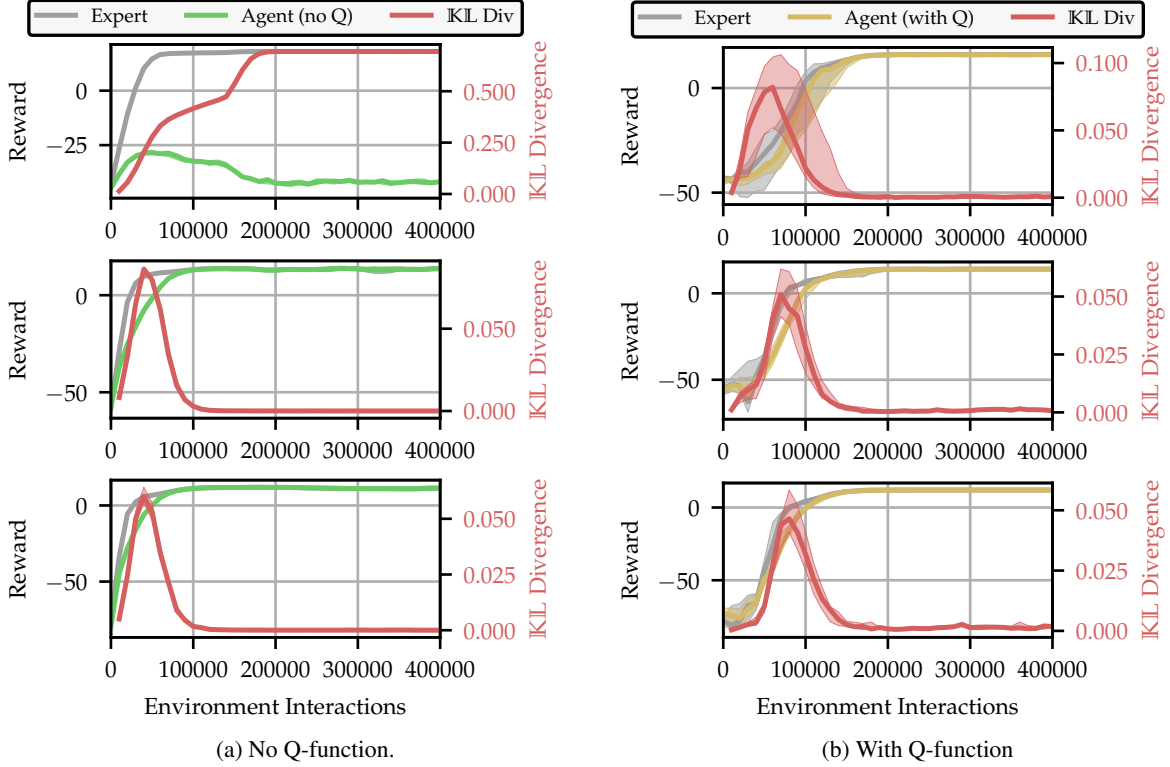


Figure 8: Results showing the performance of A2D during training when exploring one-step consistency, using a Q function or not, averaging across 10 random seeds. The top, middle and bottom rows correspond to TigerDoor-1, TigerDoor-2 and TigerDoor-3 respectively. We see that in all cases the expert learns quickly and stably. However, when a Q function is not used, the expert and agent do not converge to the same solution, as indicated by the high divergence loss in the top left figure. Convergence is slower, and the KL divergence is slightly more variable when using a Q function. This behavior leads us to suggest not learning the Q function, unless the environment is not one-step consistent.

C.2 Proof that implicit agent policy minimizes IL objective

Theorem 2 (Asymmetric IL Target, reproduced from Section 3). *For any fully observable policy π_θ and any fixed policy π_η , the implicit agent policy $\hat{\pi}_\theta^\eta$ minimizes the following asymmetric imitation learning objective:*

$$\hat{\pi}_\theta^\eta = \arg \min_{\pi \in \Pi_\Phi} \mathbb{E}_{s_t, b_t \sim d^{\pi_\eta}} [\text{KL}[\pi_\theta(a_t|s_t) || \pi(a_t|b_t)]] . \quad (10)$$

Proof. We consider a single belief state here and note that this applies for all belief states if the policy class is sufficiently expressive:

$$\pi^* = \arg \min_{\pi} \mathbb{E}_{s_t \sim d^{\pi_\eta}(s_t|b_t)} [\text{KL}[\pi_\theta(a_t|s_t) || \pi(a_t|b_t)]] , \quad \forall b_t. \quad (25)$$

Expanding the expectation and KL term:

$$\pi^* = \arg \min_{\pi} \int_{s_t} \int_{a_t} \pi_\theta(a_t|s_t) \log \left(\frac{\pi_\theta(a_t|s_t)}{\pi(a_t|b_t)} \right) da_t d^{\pi_\eta}(s_t|b_t) ds_t, \quad (26)$$

$$= \arg \min_{\pi} \int_{s_t} \int_{a_t} \pi_\theta(a_t|s_t) \log \pi_\theta(a_t|s_t) da_t d^{\pi_\eta}(s_t|b_t) ds_t - \quad (27)$$

$$\int_{s_t} \int_{a_t} \pi_\theta(a_t|s_t) \log \pi(a_t|b_t) da_t d^{\pi_\eta}(s_t|b_t) ds_t, \quad (28)$$

$$= \arg \min_{\pi} K - \int_{s_t} \int_{a_t} \pi_\theta(a_t|s_t) \log \pi(a_t|b_t) da_t d^{\pi_\eta}(s_t|b_t) ds_t, \quad (29)$$

where the term K is independent of ϕ . Manipulating the rightmost term:

$$\pi^* = \arg \min_{\pi} K - \int_{a_t} \int_{s_t} \pi_{\theta}(a_t|s_t) d^{\pi_{\eta}}(s_t|b_t) ds_t \log \pi(a_t|b_t) da_t, \quad (30)$$

$$= \arg \min_{\pi} K - \int_{a_t} \hat{\pi}_{\theta}^{\eta}(a_t|b_t) \log \pi(a_t|b_t) da_t, \quad (31)$$

We are now free to set the value of K , which we denote as K' , so long as it is independent of ϕ , as this does not alter the minimizing argument:

$$K' = \int_{a_t} \hat{\pi}_{\theta}^{\eta}(a_t|b_t) \log \hat{\pi}_{\theta}^{\eta}(a_t|b_t) da_t, \quad (32)$$

$$\pi^* = \arg \min_{\pi} K' - \int_{a_t} \hat{\pi}_{\theta}^{\eta}(a_t|b_t) \log \pi(a_t|b_t) da_t, \quad (33)$$

$$= \arg \min_{\pi} \int_{a_t} \hat{\pi}_{\theta}(a_t|b_t) \log \hat{\pi}_{\theta}(a_t|b_t) da_t - \int_{a_t} \hat{\pi}_{\theta}(a_t|b_t) \log \pi(a_t|b_t) da_t. \quad (34)$$

Combining the logarithms:

$$\pi^* = \arg \min_{\pi} \int_{a_t} \hat{\pi}_{\theta}^{\eta}(a_t|b_t) \log \left(\frac{\hat{\pi}_{\theta}^{\eta}(a_t|b_t)}{\pi(a_t|b_t)} \right) da_t, \quad (35)$$

$$= \arg \min_{\pi} \mathbb{KL} [\hat{\pi}_{\theta}^{\eta}(a_t|b_t) || \pi(a_t|b_t)], \quad \forall b_t. \quad (36)$$

Assuming that the policy class is sufficiently expressive this KL can be exactly minimized, implying:

$$\hat{\pi}_{\theta}^{\eta}(a_t|b_t) = \pi^*(a_t|b_t). \quad (37)$$

□

This proof shows that learning the agent policy (π) using imitation learning via KL minimization (as in in (10)) targets the policy defined as the implicit agent policy as in Definition (1), and hence our definition of the implicit agent policy is well founded.

C.3 Variational Agent Policy

Lemma 4 (Variational Agent Policy). *For an MDP \mathcal{M}_{Θ} and POMDP \mathcal{M}_{Φ} , and implicit agent policy $\hat{\pi}_{\theta}$ (Definition 1), if we define a variational approximation to $\hat{\pi}_{\theta}$, parameterized by ψ , denoted $\pi_{\psi} \in \hat{\Pi}_{\Phi}$, such that the following divergence is minimized:*

$$\psi^* = \arg \min_{\psi} F(\psi) = \arg \min_{\psi} \mathbb{E}_{b_t \sim d^{\hat{\pi}_{\theta}}} [\mathbb{KL} [\hat{\pi}_{\theta}(a_t|b_t) || \pi_{\psi}(a_t|b_t)]], \quad (38)$$

then an unbiased estimator for the gradient of this objective is given by the following expression:

$$\nabla_{\psi} F(\psi) = -\mathbb{E}_{s_t, b_t \sim d^{\hat{\pi}_{\theta}}} [\mathbb{E}_{a_t \sim \pi_{\theta}(a_t|s_t)} [\nabla_{\psi} \log \pi_{\psi}(a_t|b_t)]] . \quad (39)$$

Proof.

$$F(\psi) = \mathbb{E}_{b_t \sim d^{\hat{\pi}_{\theta}}(b_t)} [\mathbb{KL} [\hat{\pi}_{\theta}(a_t|b_t) || \pi_{\psi}(a_t|b_t)]], \quad (40)$$

$$= \mathbb{E}_{b_t \sim d^{\hat{\pi}_{\theta}}(b_t)} \left[\int_{a_t \in \mathcal{A}} \log \frac{\hat{\pi}_{\theta}(a_t|b_t)}{\pi_{\psi}(a_t|b_t)} \hat{\pi}_{\theta}(a_t|b_t) da_t \right], \quad (41)$$

$$= \int_{b_t \in \mathcal{B}} \int_{a_t \in \mathcal{A}} -\log \pi_{\psi}(a_t|b_t) \hat{\pi}_{\theta}(a_t|b_t) da_t d^{\hat{\pi}_{\theta}}(b_t) db_t + C, \quad (42)$$

$$= - \int_{b_t \in \mathcal{B}} \int_{a_t \in \mathcal{A}} \log \pi_{\psi}(a_t|b_t) \int_{s_t \in \mathcal{S}} \pi_{\theta}(a_t|s_t) p_{\hat{\pi}_{\theta}}(s_t|b_t) ds_t da_t p_{\hat{\pi}_{\theta}}(b_t) db_t + C, \quad (43)$$

$$= - \int_{b_t \in \mathcal{B}} \int_{a_t \in \mathcal{A}} \int_{s_t \in \mathcal{S}} \log \pi_{\psi}(a_t|b_t) \pi_{\theta}(a_t|s_t) p_{\hat{\pi}_{\theta}}(s_t, b_t) ds_t da_t db_t + C, \quad (44)$$

$$= -\mathbb{E}_{s_t, b_t \sim d^{\hat{\pi}_{\theta}}(s_t, b_t)} \left[\int_{a_t \in \mathcal{A}} \log \pi_{\psi}(a_t|b_t) \pi_{\theta}(a_t|s_t) da_t \right] + C, \quad (45)$$

$$= -\mathbb{E}_{s_t, b_t \sim d^{\hat{\pi}_{\theta}}(s_t, b_t)} [\mathbb{E}_{a_t \sim \pi_{\theta}(a_t|s_t)} [\log \pi_{\psi}(a_t|b_t)]] + C, \quad (46)$$

$$\nabla_{\psi} F(\psi) = -\mathbb{E}_{s_t, b_t \sim d^{\hat{\pi}_{\theta}}(s_t, b_t)} [\mathbb{E}_{a_t \sim \pi_{\theta}(a_t|s_t)} [\nabla_{\psi} \log \pi_{\psi}(a_t|b_t)]] . \quad (47)$$

□

Note here that θ is held constant in this step, and is updated in the alternate step.

Lemma 5 (Fixed Point Variational Inference Objective). *For an MDP \mathcal{M}_Θ and POMDP \mathcal{M}_Φ , and implicit agent policy $\hat{\pi}_\theta$ defined as in Definition 1, if we define a variational approximation to $\hat{\pi}_\theta$, parameterized by ψ , where $\pi_\psi \in \pi_\psi$ that minimizes the following:*

$$\psi_1^* = \arg \min_{\psi} \mathbb{E}_{b_t \sim d^{\pi_\psi}(b_t)} [\mathbb{KL} [\hat{\pi}_\theta(a_t|b_t) || \pi_\psi(a_t|b_t)]] . \quad (48)$$

If we assume that π_ψ is sufficiently expressive, such that

$$\min_{\psi} \mathbb{E}_{b_t \sim d^{\pi_\psi}(b_t)} [\mathbb{KL} [\hat{\pi}_\theta(a_t|b_t) || \pi_\psi(a_t|b_t)]] = 0 \quad (49)$$

Then we have that,

$$\psi_1^* = \psi_2^* = \arg \min_{\psi} \mathbb{E}_{b_t \sim d^{\hat{\pi}_\theta}(b_t)} [\mathbb{KL} [\hat{\pi}_\theta(a_t|b_t) || \pi_\psi(a_t|b_t)]] . \quad (50)$$

Proof. By way of contradiction, assume that there exists some t such that $d^{\hat{\pi}_\theta}(b_t, s_t) \neq d^{\pi_\psi}(b_t, s_t)$ but we have that:

$$\min_{\psi} \mathbb{E}_{b_t \sim d^{\pi_\psi}(b_t)} [\mathbb{KL} [\hat{\pi}_\theta(a_t|b_t) || \pi_\psi(a_t|b_t)]] = 0. \quad (51)$$

Then we can first note inductively, that because the initial state / observation distribution is independent of the policy, that necessarily $d^{\hat{\pi}_\theta}(b_0, s_0) = d^{\pi_\psi}(b_0, s_0)$. What's more, based upon our assumption above, this implies:

$$\arg \min_{\psi} \mathbb{E}_{b_0 \sim d^{\pi_\psi}(b_0)} [\mathbb{KL} [\hat{\pi}_\theta(a_0|b_0) || \pi_\psi(a_0|b_0)]] = \arg \min_{\psi} \mathbb{E}_{b_0 \sim d^{\hat{\pi}_\theta}(b_0)} [\mathbb{KL} [\hat{\pi}_\theta(a_0|b_0) || \pi_\psi(a_0|b_0)]] \quad (52)$$

This means that we have that $s_0, b_0, a_0 \sim d^{\hat{\pi}_\theta}(b_0, s_0) \hat{\pi}_\theta(a_0|b_0) = s_0, b_0 \sim d^{\pi_\psi}(b_0, s_0) \pi_\psi(a_0|b_0)$ which implies that the resulting distribution over b_1, s_1 must again be equivalent for both the target and variational distribution. If we take this logic to step $t-1$, then we have that $s_{t-1}, b_{t-1} \sim d^{\hat{\pi}_\theta}(b_{t-1}, s_{t-1}) = s_{t-1}, b_{t-1} \sim d^{\pi_\psi}(b_{t-1}, s_{t-1})$. Again we can, by assumption minimize the KL divergence in action space under the expected $b_{t'}, s_{t'}$ for all t' from 0 to $t-1$. Which would imply that for the resulting distribution over s_t, b_t for the next time step must also be the same, however this contradicts our assumption regarding the b_t, s_t . Thus under the assumptions stated above, we have that ψ_1^* and ψ_2^* are equal. \square

C.4 Updating the Agent

Theorem 6 (Agent-conditional Expert Update). *For an expert policy, π_θ , and an agent policy learned through KL-minimization, π_ψ , targeting the implicit agent policy, $\hat{\pi}_\theta$, the policy gradient update can be transformed into a policy gradient update applied to the expert:*

$$\nabla_\theta J_\psi(\theta) = \nabla_\theta \mathbb{E}_{a_t, b_t \sim \hat{\pi}_\theta(a_t|b_t) d^{\pi_\psi}(b_t)} [Q^{\hat{\pi}_\theta}(a_t, b_t)] , \quad (53)$$

$$= \mathbb{E}_{s_t, b_t \sim d^{\pi_\psi}(s_t, b_t)} [\mathbb{E}_{a_t \sim \pi_\theta(a_t|s_t)} [Q^{\hat{\pi}_\theta}(a_t, b_t) \nabla_\theta \log \pi_\theta(a_t|s_t)]] , \quad (54)$$

Proof.

$$\nabla_\theta J_\psi(\theta) = \nabla_\theta \mathbb{E}_{a_t, b_t \sim \hat{\pi}_\theta, d^{\pi_\psi}} [Q^{\hat{\pi}_\theta}(a_t, b_t)] , \quad (55)$$

$$= \nabla_\theta \int_{b_t} \int_{a_t} Q^{\hat{\pi}_\theta}(a_t, b_t) \hat{\pi}_\theta(a_t|b_t) da_t d^{\pi_\psi}(b_t) db_t, \quad (56)$$

$$= \nabla_\theta \int_{b_t} \int_{a_t} Q^{\hat{\pi}_\theta}(a_t, b_t) \int_{s_t} \pi_\theta(a_t|s_t) d^{\pi_\psi}(s_t|b_t) ds_t da_t d^{\pi_\psi}(b_t) db_t, \quad (57)$$

$$= \nabla_\theta \int_{s_t} \int_{b_t} \int_{a_t} Q^{\hat{\pi}_\theta}(a_t, b_t) \pi_\theta(a_t|s_t) d^{\pi_\psi}(s_t, b_t) da_t ds_t db_t, \quad (58)$$

$$= \mathbb{E}_{s_t, b_t \sim d^{\pi_\psi}(s_t, b_t)} \left[\nabla_\theta \int_a Q^{\hat{\pi}_\theta}(a_t, b_t) \pi_\theta(a_t|s_t) da \right] , \quad (59)$$

$$= \mathbb{E}_{s_t, b_t \sim d^{\pi_\psi}(s_t, b_t)} [\nabla_\theta \mathbb{E}_{a_t \sim \pi_\theta(a_t|s_t)} [Q^{\hat{\pi}_\theta}(a_t, b_t)]] , \quad (60)$$

$$= \mathbb{E}_{s_t, b_t \sim d^{\pi_\psi}(s_t, b_t)} [\mathbb{E}_{a_t \sim \pi_\theta(a_t|s_t)} [Q^{\hat{\pi}_\theta}(a_t, b_t) \nabla_\theta \log \pi_\theta(a_t|s_t)]] , \quad (61)$$

\square

D Experimental Configurations

For both gridworld experiments, the image is rendered as a 42×42 RGB image. The agent has four actions available, moving in each of the compass directions. Each movement incurs a reward of -2 , hitting the weak patch of ice or tiger incurs a reward of -100 , and reaching the goal incurs a reward of 20 . Pushing the button in Tiger Door is free, but effectively costs 4 due to its position, or 2 in the one step consistency experiments. Policy performance is evaluated every 5 steps by sampling 2000 interactions under the stochastic policy. A discount factor of $\gamma = 0.995$ was used, $\lambda = 0.95$ in the GAE calculation. A hard time horizon of $T = 200$ is used.

For the expert we use a two layer MLP, with 64 hidden units in each layer, outputting the log-probabilities of each action. Agent policies use a two layer convolutional policy, each with 32 filters, mapping to a flat hidden state with 50 hidden units, being used as input into a two layer MLP, each with 64 hidden units, outputting the log-probabilities of each action. In TRPO, the expert policy is updated using a trust region allowing a maximum KL-divergence of 0.01 . The value function is a two layer MLP, each with 64 hidden units, targeting the sum of rewards ahead by minimizing the mean squared error. 32 batches are constructed from the rollout and 10 epochs are applied to the value function at each step, and updated using ADAM with a learning rate of $7e - 4$. L2 regularization is applied to all networks, with a coefficient of 0.001 .

The expert policy used in AD is the result of applying TRPO on the MDP using the above hyperparameters. We find that the MDP converges within approximately $80,000$ environment interactions, and so we begin the AD line at this value. For both A2D and AD, a replay buffer of size $5,000$ was used. The KL-divergence between the expert and agent action distributions is minimized by performing stochastic gradient descent, using ADAM with a learning rate of $3e - 4$, using a batch size of 64 . In AD, β is annealed to zero after the first time step (as recommended by Ross et al. (2011)). For the experiments in Figure 4, an entropy regularizer is applied directly to the advantages computed, with coefficient 10 . For the experiments in Figure 5 an entropy regularizer of 0.001 is applied directly to the surrogate loss. We did not find either one of these configurations to be noticeably more effective. Asymmetric reinforcement learning takes the compact and omniscient state representation (s_t) as input. When training the encoder, we rollout under a trained MDP, collect the trajectories generated by $10,000$ environment interactions. An encoder that takes the images as input and targets the true state is learned by regressing the predictions on to the true state. We also start this curve at the $80,000$ interactions required to train the expert from which the encoder is learned. We confirm for both pretrained encoders and AD that the policy and encoder class can represent the required policies and transforms when conditioned on fully observed image-based input.

For investigating the use of Q-function approximators, we use a lambda value of zero to rely on the function approximators. Q-functions are learned using the same method as value functions, except target the expected sum of rewards ahead conditioned on both state and action with a learning rate $3e - 4$. We also use TRPO with a trust region KL-divergence of 0.001 . In the PPO experiments in Figure 7 we use a batch size of 32 and a learning rate of $7e - 4$ when updating the policy. We also decay β as a faster rate of 0.8 .

E Additional Related Work

We now present a comprehensive review of existing literature not already covered. Exploiting asymmetric learning to accelerate learning has been explored in numerous previous work under a number of different frameworks, application domains, and levels of theoretical analysis.

The notion of using fully observed states unavailable at deployment time is often referred to as exploiting “privileged information” (Vapnik & Vashist, 2009; Lambert et al., 2018). For clarity, we refer to the expert as having access to privileged information, and the agent as only having access to a partial observation. We note that the use of the term “expert” does not imply that this policy is necessarily optimal under the MDP. Indeed, in A2D, the expert is co-trained with the agent, such that the expert is approximately a uniform random distribution at the start of the learning procedure. The term privileged information is more general than simply providing the world state, and may include additional loss terms or non-trivial transforms of the world state that expedite learning the agent. In this work, we exclusively consider the most general scenario where the privileged information is the full world state. However, there is nothing precluding defining an extended state space to include hand-designed features extracted from the state, or, using additional, hand crafted reward shaping terms when learning (or adapting) the expert.

E.1 Encodings

The first use-case we examine is probably the simplest, and the most widely studied. Asymmetric information is used to learn an encoding of the observation that reduces the dimensionality while retaining information. Standard

reinforcement learning approaches are then employed freezing this encoding. Two slight variations on this theme exist. In the first approach, an MDP policy is learned to generate rollouts conditioned on omniscient information, and an encoder is learned on state-observation pairs visited during these rollouts (Levine et al., 2016; Finn et al., 2016). Either the encoder acts to directly recover the underlying states, or simply learns a lower-dimensional embedding where performing reinforcement learning is more straightforward.

Andrychowicz et al. (2020) explore learning to manipulate objects using a mechanical hand using *both* state information from the robot (joint poses, fingertip positions etc) and RGB images. This particular application is an interesting hybrid approach dictated by the domain. State information pertaining to the manipulator is easily obtained, but state information about the pose of the object being manipulated is unavailable and must be recovered using the images. A controller is learned in simulation (MDP), while simultaneously (and separately from the MDP) a separate perception network is learned that maps the image to the pose of the object being manipulated. State information and pose encoding are then concatenated and used as the state vector on which the policy acts. While the pose of the object is unobserved, it is readily recoverable from a single frame (or stack of frames), and hence the partial observation is predominantly a high-dimensional and bijective embedding of the true state. If the true position of the hand was not available, this would be less certain as the object and other parts of the manipulator obfuscates much of the manipulator from any of the three viewpoints (more viewpoints would of course reverse this to being a bijection). The use of a recurrent policy further improves the recovery of state as only the innovation in state needs to be recovered.

E.2 Asymmetric values

Another well-explored use-case is to instead exploit asymmetric information for to improve learning a value or Q-function (Könönen, 2004; Pinto et al., 2017; Andrychowicz et al., 2020). This is achieved by conditioning either the value function or Q-function on different information than the policy that is either more informative, or lower dimensional representations, and can help guide learning (Könönen (2004); Pinto et al. (2017)). Learning the value or Q function in a lower-dimensional setting enables this function to be learned more stably and with fewer samples, and hence can track the current policy more effectively. Since the value and Q-function are not used at test time, there is no requirement for privileged information to be available when deployed. Pinto et al. (2017) introduce this in a robotics context, using an asymmetric value function, conditioned on the true underlying state of a robotic manipulator, to learn a partially observing agent conditioned only on a third-person monocular view of the arm. Similar ideas were explored previously by Könönen (2004) in relation to semi-centralized multi-agent systems, where each agent only partially observes the world state, but a central controller is able to observe the whole state. The state used by the central controller is used to evaluate the value of a particular world state, whilst each agent only acts on partial information.

E.3 Cloning

Behavioral cloning and imitation learning (Kang et al., 2018; Ross et al., 2011), introduced above in Section 2, is, in our opinion, an under-explored avenue for expediting learning in noisy and high-dimensional partially observed processes. The main observation is that this process separates learning to act and learning to perceive (Chen et al., 2020). The fully observing expert learns to act, without the presence of extraneous patterns or noise. The agent then learns to perceive such that it can replicate the actions of the expert. A major benefit of cloning approaches is that perception is reduced to a supervised learning task, with lower variance than the underlying RL task.

Pinto et al. (2017) also briefly assess using asymmetric DAGger as a baseline. It is observed that the agent learns quickly, but actually converges to a worse solution than the asymmetric actor-critic solution. This difference is attributed to the experts access to (zero variance) state information otherwise unavailable to the partially observing agent. Our work builds on this observation, seeking to mitigate such weaknesses. Surprisingly, and to the best of our knowledge, no work (including Pinto et al. (2017)) has provided an in-depth analysis of this method, or directly built off this idea. Subsequent work, such as the method present by Sun et al. (2018), use RL in an imitation learning framework to gain performance beyond that of the expert, however, they do not explicitly address updating the expert.

Chen et al. (2020) showed that large performance gains can be found in an autonomous vehicles scenario by using IL through the use of an asymmetric expert, specifically for learning to drive in the autonomous vehicle simulator CARLA (Dosovitskiy et al., 2017). Chen et al. (2020) train an expert from trajectories, created by human drivers, using behavioral cloning conditioned on an encoded aerial rendering of the environment including privileged information unavailable to the agent at deployment time. The aerial rendering facilitates extensive data augmentation schemes that would otherwise be difficult, or impossible, to implement in a symmetric setting. The agent is then learned using DAGger-based imitation learning. However, this general approach implicitly makes assumptions about the performance of the expert, as well as the underlying consistency (as we define in Section 3) between the underlying fully and partially observed Markov decision processes.

E.4 Co-learning Expert and Agent

The most recent work (some of which is concurrent with our work) investigates co-training of the agent and expert. This builds on the AD approach, as introduced above (c.f. Pinto et al. (2017)) where instead of assuming the expert exists and simply projected onto the agent, the expert and agent policies are learned simultaneously, where an additional training phase is added to “align” the expert and agent (Salter et al., 2019; Song et al., 2019), architectural modification (Kamienny et al., 2020), or both (Schwab et al., 2019).

Salter et al. (2019) trains separate policies for agent and expert using spatial attention, where the expert is conditioned on the state of the system, and the agent is conditioned on a monocular viewpoint. By inspecting the attention map of expert and agent, it is simple to establish what parts of the state or image the policy is using to act. An auxiliary (negative) reward term is added to the reward function that penalizes differences in the attention maps, such that the agent and expert are regularized to use the same underlying features. This auxiliary loss term transfers information from the MDP to the POMDP. The main drawbacks of this approach however are its inherent reliance on an attention mechanism, and tuning the hyperparameters dictating the weight of having a performant agent, expert and the level of alignment between the attention mechanisms. Further, using an attention as the transfer mechanism between the agent and expert somewhat introduces an additional layer of complexity and obfuscation of the actual underlying mechanism of information transfer.

Song et al. (2019) present an algorithm, CoPiEr, that co-trains two policies, conditioned on different information (any combination of fully or partially observing). CoPiEr rolls out under both policies separately, and then selects the rollouts from the policy that performs the best. These samples are then used in either an RL or IL (or hybrid of the two) style update. In this sense, the better performing policy (with ostensibly “better” rollouts) provides high-quality supervision to the policy with lower quality rollouts. MDP to POMDP transfer or privileged information is not considered. Most significantly, imitation learning is proposed as a method of transferring from one policy to another, or, RL augmented with an IL loss to provide better supervision while retaining RLs capability to explore policy space.

Schwab et al. (2019) on the other hand extend Pinto et al. (2017) by introducing multitask reinforcement learning themes. A “task” is uniquely described by the set of variables that the policy is conditioned on, such as images from different view points, true state information and proprioceptive information. An input-specific encoder encodes each observation before mixing the encoded input features and passing these to a head network which outputs the actions. Instead of aligning attention mechanisms (as per Salter et al. (2019)), Schwab et al. (2019) the head network is shared between tasks providing alignment between the single-input policies. At test time, only those observations that are available need to be supplied to the policy, respecting the partial observability requirement at test time. This approach does not explicitly use an expert, instead using a greater range of more informative information channels to efficiently learn the policy head, while simultaneously co-training the channel-specific encoders.

Finally, the work of Kamienny et al. (2020) present privileged information dropout (PI-D). The general approach of information dropout (Achille & Soatto, 2018) is to learn a model while randomly perturbing the internal state of the model, effectively destroying some information. The hypothesis is that this forces the model to learn more robust and redundant features that can survive this corruption. Kamienny et al. (2020) use this theme by embedding both partial observation and state, where the state embedding is then used to corrupt (through multiplicative dropout) the internal state of the agent. The PI expert is then able to mask uninformative patterns in the observations (using the auxiliary state information), facilitating more efficient learning. The PI can then be easily marginalized out by not applying the dropout term. Importantly however, reinforcement learning is still performed in the partially observing agent, a characteristic we wish to avoid due to the high-variance nature of this learning.